



Article

HPLC Study of Product Formed in the Reaction of NBD-Derived Fluorescent Probe with Hydrogen Sulfide, Cysteine, *N*-acetylcysteine, and Glutathione

Daniel Słowiński ¹ , Małgorzata Świerczyńska ¹, Jarosław Romański ² and Radosław Podsiadły ^{1,*} 

¹ Institute of Polymer and Dye Technology, Faculty of Chemistry, Lodz University of Technology, Stefanowskiego 16, 90-537 Lodz, Poland

² Department of Organic and Applied Chemistry, Faculty of Chemistry, University of Lodz, Tamka 12, 91-403 Lodz, Poland

* Correspondence: radoslaw.podsiadly@p.lodz.pl

Abstract: Hydrogen sulfide (H₂S) and its bioderivatives analogs, such as L-cysteine (L-Cys) and glutathione (GSH), are ubiquitous biological thiols in the physiological and pathological processes of living systems. Their aberrant concentration levels are associated with many diseases. Although several NBD-based fluorescence probes have been developed to detect biological thiols, the HPLC-detection of H₂S, GSH, L-Cys, and *N*-acetylcysteine-specific products has not been described. Herein, a novel NBD-derived pro-coumarin probe has been synthesized and used to develop a new strategy for the triple mode detection of H₂S and such thiols as GSH, L-Cys, and NAC. Hydrogen sulfide and those biothiols at physiological pH release fluorescent coumarin from the probe and cause a significant fluorescence enhancement at 473 nm. The appropriate NBD-derived product for H₂S, L-Cys, GSH, and NAC has a different color and retention time that allows distinguishing these biological thiols meaning the probe has a great possibility in the biological application. Fluorescent imaging combined with colorimetric and HPLC detection of H₂S/biothiol-specific product(s) brings a potential tool for confirming the presence of biological thiols and determining concentrations in various aqueous biological samples.

Keywords: biothiols detections; markers; coumarin-derived probe; hydrogen sulfide; fluorescent probe; colorimetric probe



Citation: Słowiński, D.; Świerczyńska, M.; Romański, J.; Podsiadły, R. HPLC Study of Product Formed in the Reaction of NBD-Derived Fluorescent Probe with Hydrogen Sulfide, Cysteine, *N*-acetylcysteine, and Glutathione. *Molecules* **2022**, *27*, 8305. <https://doi.org/10.3390/molecules27238305>

Academic Editor: Lucia Panzella

Received: 4 November 2022

Accepted: 25 November 2022

Published: 28 November 2022

Publisher's Note: MDPI stays neutral with regard to jurisdictional claims in published maps and institutional affiliations.



Copyright: © 2022 by the authors. Licensee MDPI, Basel, Switzerland. This article is an open access article distributed under the terms and conditions of the Creative Commons Attribution (CC BY) license (<https://creativecommons.org/licenses/by/4.0/>).

1. Introduction

Hydrogen sulfide (H₂S), L-cysteine (L-Cys), homocysteine (Hcy), and glutathione (GSH) are the most common small molecular biological thiols [1]. They are closely related and have essential distinct biological and pharmacological roles in many processes [2]. Hydrogen sulfide plays a vital and physiological function in the human body [3]. That small molecule, although commonly recognized as toxic gas and environmental hazard, is now accepted as a critical, endogenously produced signaling mediator, similar to carbon monoxide (CO) and nitric oxide (NO) [4,5]. Hydrogen sulfide rapidly travels through cell membranes without additional transporters and does not have one single pathway- it affects multiple cellular effectors in a cell or tissue-dependent manner [6]. In humans, the concentration of H₂S in the body can differ according to age, the kind of tissues, and measuring methods. For example, the level of H₂S in the peripheral blood is generally 30–100 μM, while the H₂S level in the mammalian brain is 50–160 μmol/L [7,8]. According to current research, cells produce H₂S via the enzymatic activity of cystathionine-γ-lyase (CSE) and cystathionine-β-synthase (CBS) [9]. Besides this synthetic pathway, H₂S is also produced by the activity combination of the cysteine aminotransferase (CAT) and 3-mercaptopyruvate sulfurtransferase (MST) [10], and can also be made endogenously through nonenzymatic pathways.

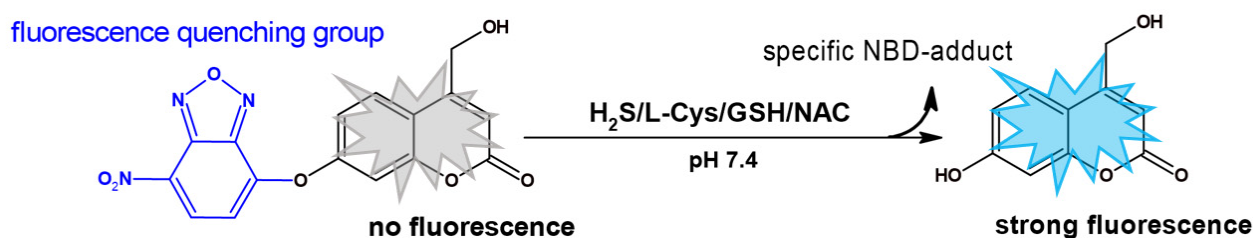
The glycolytic pathway can reduce thiosulfate, thiocysteine, and other sulfur-containing molecules in the blood to H₂S [11].

Hydrogen sulfide is related to many physiological processes, including vasodilation, neurotransmission, angiogenesis, inhibition of insulin signaling, antioxidation, and regulation of blood vessel tone. It can also effectively neutralize reactive oxygen and nitrogen species (ROS and RNS) [12–18]. In recent years, treatment of myocardial ischemia injury with H₂S has emerged as a novel and promising strategy to protect cardiac structure and function. It was reported that H₂S could directly increase the production of reduced glutathione (GSH) to affect cytoprotective effects against ROS-mediated damage [19]. However, abnormal levels of H₂S are associated with human health and many diseases [20], such as diabetes [21,22], arterial and pulmonary hypertension [23], gastric mucosal damage [24], liver cirrhosis [25,26], ischemia [27], and Alzheimer's disease [28,29].

In the last decade, some analytical methods (gas chromatography, methylene blue assay, sulfur-selective electrodes) were developed for H₂S detection, but they are unsuitable for in situ analysis [30,31]. In contrast to traditional methods, techniques based on fluorescent probes could maintain better accuracy and efficiency, higher selectivity and sensitivity, and noninvasive real-time imaging [32]. Based on nucleophilic addition [33], reduction of azide or nitro group to amine [34], copper sulfide precipitation reaction [35], and thiolysis of ethers [36–38], a wide range of reaction-based H₂S-specific probes have been developed and applied in living biological systems. In the H₂S-induced thiolysis reaction, the design strategy of the H₂S fluorescent probes is based on hydrosulfide anion (HS[−]) selectively attacking a single electrophilic position on the probe scaffold, which is followed by the removal of electrophilic functionalities to generate fluorescent signals. The fluorescence of these probes is typically protected with an incorporated strong electron-withdrawing group such as naphthoquinone [39] or nitrobenzofuran (NBD) that can be cleaved in the presence of H₂S [40]. Probes derived from NBD moiety are widely applied in biological applications due to their small size and good photophysical properties in aqueous systems [41].

Nevertheless, most reported probes suffered from limitations such as narrow Stokes shift (<60 nm) or a long response time. Additionally, many probes cannot distinguish H₂S from other biothiols because they all contain a sulfhydryl group with similar nucleophilic properties [42]. Therefore, searching for an effective tool capable of simultaneously monitoring the level of H₂S in vivo, along with the possibility of distinguishing selected thiols, is a significant challenge. Although several NBD-based fluorescence probes have been developed to detect biothiols, the HPLC-detection of NBD-derived specific products for H₂S, GSH, Cys, or NAC has not been characterized.

In this report, we describe the design of a novel fluorescent probe (NBD-O-CmCH₂OH) consisting of a fluorophore of 7-hydroxy-4-(hydroxymethyl)-2H-chromen-2-one (CmCH₂OH) connected via ether linkage with 7-nitrobenz-2-oxa-1,3-diazole (NBD) moiety. Treatment of this probe with H₂S or biothiols rapidly cleaved the C-O bond to afford coumarin fluorophore and the diagnostic marker products of H₂S, Cys, GSH, and NAC, easily detected by HPLC (Scheme 1). Moreover, these specific products have different spectral characteristics, resulting in different solutions' colors. Therefore, combining non-invasive fluorescence/colorimetric monitoring with HPLC analyses to detect H₂S/biothiols-specific products will provide more detailed information on the species identity.

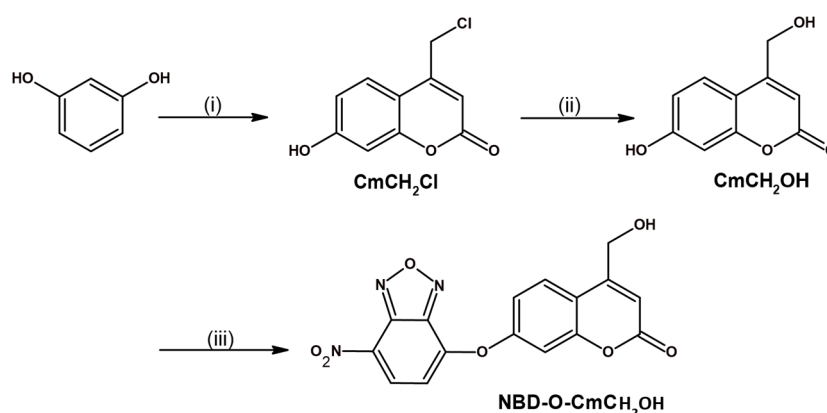


Scheme 1. Probe NBD-O-CmCH₂OH and proposed reaction with biothiols.

2. Results and Discussion

2.1. Synthesis of the Probe and H₂S/Biothiols-Specific Product

First, we designed and synthesized a pro-coumarin NBD-derived probe to develop the strategy for triple mode detection of H₂S and biothiols (GSH, Cys, NAC). Previously reported NBD-coumarin probes [43–47] were used in aqueous solutions with the addition of a large amount (above 30% *v/v*) of organic co-solvent. To improve the probe's solubility, we choose fluorophore 7-hydroxy-4-(hydroxymethyl)-2H-chromen-2-one (CmCH₂OH) with an additional hydroxyl group. The probe was obtained using the three-step route with a good yield (Scheme 2). 4-Chloromethyl-7-hydroxycoumarin CmCH₂Cl was synthesized from commercially available ethyl (2-chloroaceto)acetate and resorcinol [48]. Next, the product was converted into fluorophore CmCH₂OH [49]. Finally, the probe NBD-O-CmCH₂OH in 69% yield was prepared by coupling CmCH₂OH with NBD-Cl in the presence of triethylamine.

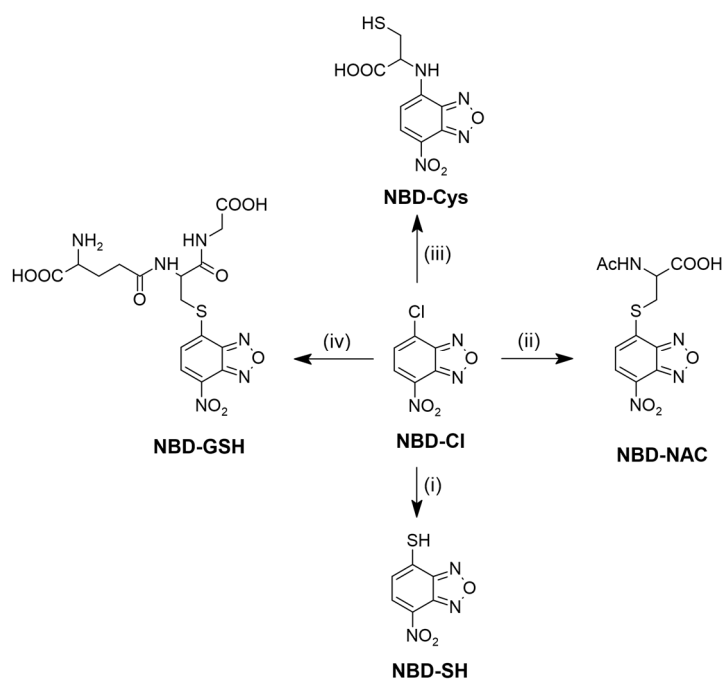


Scheme 2. Synthesis of probe NBD-O-CmCH₂-OH. Reagents and conditions: (i) ethyl 4-chloroacetoacetate, H₂SO₄, 5 °C, 2 h; (ii) water, reflux, 48 h; (iii) NBD-Cl, Et₃N, room temperature, 8 h.

7-nitrobenzo[c][1,2,5]oxadiazole-4-thiol (NBD-SH) was synthesized from NBD-Cl and sodium sulfide. Biothiols-specific products, 7-nitrobenzo[c][1,2,5]oxadiazole-4-glutathione (NBD-GSH), 7-nitrobenzo[c][1,2,5]oxadiazole-4-cysteine (NBD-Cys), *N*-acetyl-S-(7-nitrobenzo[c][1,2,5]oxadiazol-4-yl)cysteine (NBD-NAC) were obtained by mixing NBD-Cl with an excess of proper biothiol (Scheme 3) at room temperature in the presence of triethylamine. The structure of all synthesized products was confirmed by ¹H NMR, ¹³C NMR, and HRMS spectroscopy (see Supplementary Materials, Figures S6–S25). The absorbance and emission profiles of CmCH₂OH, probe, and NBD-Cl are illustrated in Figure S1.

2.2. Spectral Response of NBD-O-CmCH₂OH toward Na₂S and Biothiols

Several coumarin-based compounds containing the NBD moiety as the sensing group have been used as fluorescent probes for the thiol species (GSH, Cys, Hcy, H₂S) [43–47]. In our research, we also decided to test the reactivity of the probe toward the cysteine pro-drug, *N*-acetylcysteine (NAC). Our results in Figures 1 and S2 confirmed that studied sulfhydryl compounds could release the fluorescent coumarin from NBD-O-CmCH₂OH. The fluorescent signal reaches a plateau within 10 min in phosphate buffer (PB buffer) containing 10% acetonitrile (MeCN) (*v/v*). The time-dependent fluorescence at 473 nm was used to determine reaction kinetics. The pseudo-first-order rates (*k*_{obs}) were found by fitting the data with a single exponential function (Figure S2). The determined kinetic parameters (Table 1) also show that the tested probe reacts with thiols at similar rate constants. These results indicated that the NBD-based probe could respond efficiently with micromolar-tested biothiols under physiological conditions.



Scheme 3. Synthesis of NBD-derived compounds. Reagents and conditions: (i) Na_2S , MeOH, room temperature, 0.5 h; (ii) NAC, EtOH/ H_2O 4:1 (*v/v*), room temperature, 3 h; (iii) L-Cys, EtOH/ H_2O 4:1 (*v/v*), room temperature, 3 h; (iv) GSH, EtOH/ H_2O 4:1 (*v/v*), room temperature, 3 h.

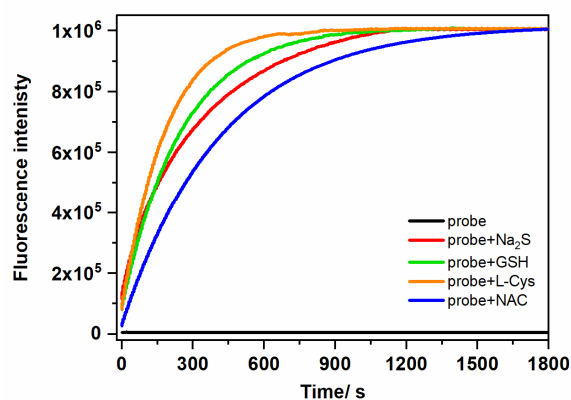


Figure 1. The time-dependent fluorescence intensity at 473 nm for NBD-O-CmCH₂OH (5 μM) in the absence or the presence of various thiol species (50 μM) in PB buffer (0.1 M, pH 7.4, containing 10% MeCN, *v/v*).

Table 1. Rate constants and limit of detection for reactions of hydrogen sulfide and the low-molecular-weight thiols cysteine, *N*-acetyl-L-cysteine, and glutathione with the studied probe.

	k_{obs} (10^3 s^{-1})	LOD (nM)
H_2S (pK_a 7.0 ^a)	3.02	140
GSH (pK_a 8.66 ^b)	4.00	60
L-Cys (pK_a 8.33 ^b)	5.64	26
NAC (pK_a 9.43 ^c)	2.5	32

^a from [50]; ^b from [51]; ^c from [52].

Next, we investigated the colorimetric responses of NBD-O-CmCH₂OH in the absence and presence of thiol species. The electronic absorption spectra recorded after the bolus addition of sulfhydryl compounds are presented in Figure 2.

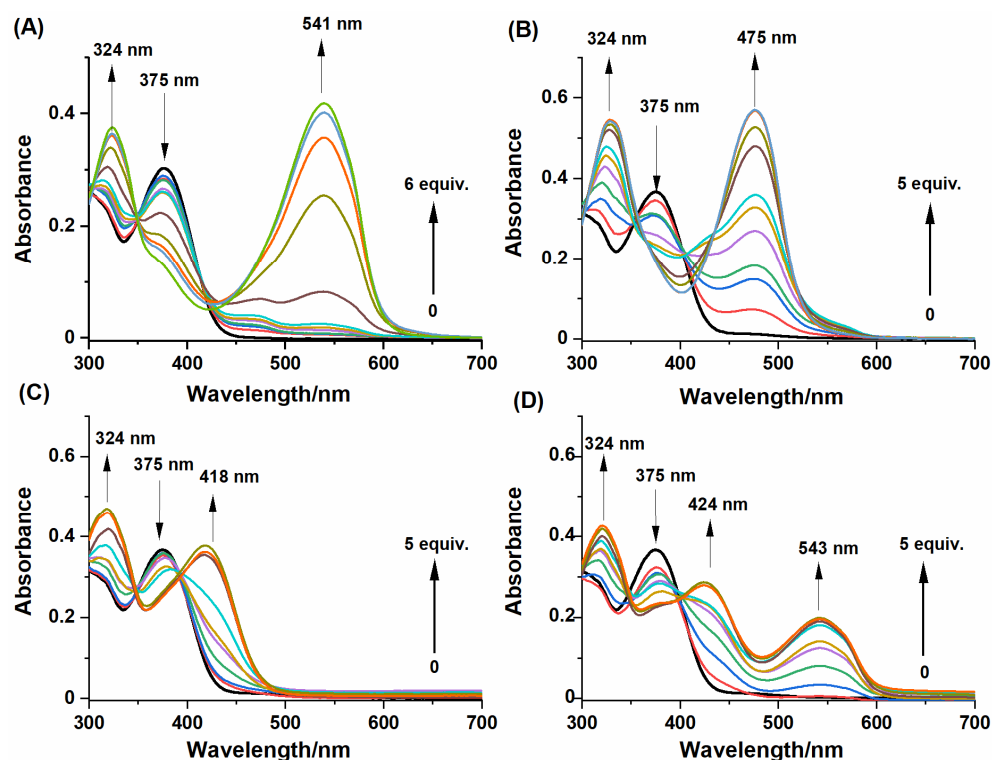


Figure 2. Absorption spectral changes of NBD-O-CmCH₂OH (30 μM) responses to various concentrations of (A) Na₂S (0–180 μM); (B) L-Cys (0–150 μM); (C) GSH (0–150 μM), (D) NAC (0–150 μM) in PB buffer (0.1 M, pH 7.4, with 10% MeCN, *v/v*). Spectra were recorded after 10 min of incubation at room temperature.

As shown in Figure 2, the probe (dark line) displayed an absorption peak at 375 nm. A common feature was that an absorption peak at 324 nm was observed after treatment of NBD-O-CmCH₂OH with Na₂S and biothiols. Moreover, the reaction between NBD-O-CmCH₂OH and thiol species led to a new absorption band(s) located at the wavelength listed in Table 2. Based on the previous articles [44,46], the individual absorption bands were assigned to the specific products formed during the reaction between thiols and probe. Reaction with: (i) Na₂S gave NBD-SH, (ii) L-Cys formed NBD-Cys adduct exhibiting the absorption of 475 nm consistent with the formation of amino-bound NBD, (iii) GSH generated NBD-GSH compound with the absorption of 418 nm consistent with the formation of sulfur-bound NBD and (iv) NAC formed NBD-NAC adduct with the absorption bands centered at 424 and 543 nm.

Table 2. Characteristic absorption bands and retention times of thiol-specific products formed in the reaction of NBD-O-CmCH₂OH with H₂S, GSH, L-Cys, and NAC.

Thiol-Specific Product	λ_{\max} (nm)	Retention Time (min)
NBD-SH	541	2.99
NBD-GSH	418	2.50
NBD-Cys	475	3.45
NBD-NAC	543, 424	3.25

The results show that the colorimetric analysis of single biothiols can give satisfactory results. NBD-coumarin probe can differentiate H₂S from GSH, L-Cys, and NAC, or sulfur species (S₂O₄²⁻, SO₃²⁻, HSO₃⁻), when only single components were analyzed (Figure 3). However, in a mixture of thiol species, their colorimetric identification may lead to wrong conclusions, especially when we intend to study in this way the influence of NAC on the level of GSH, H₂S, or L-Cys. In addition, we compared the change in fluorescence

intensity during the reaction of NBD-Cl with analytes and the probe NBD-O-CmCH₂OH with analytes (Figure S4).

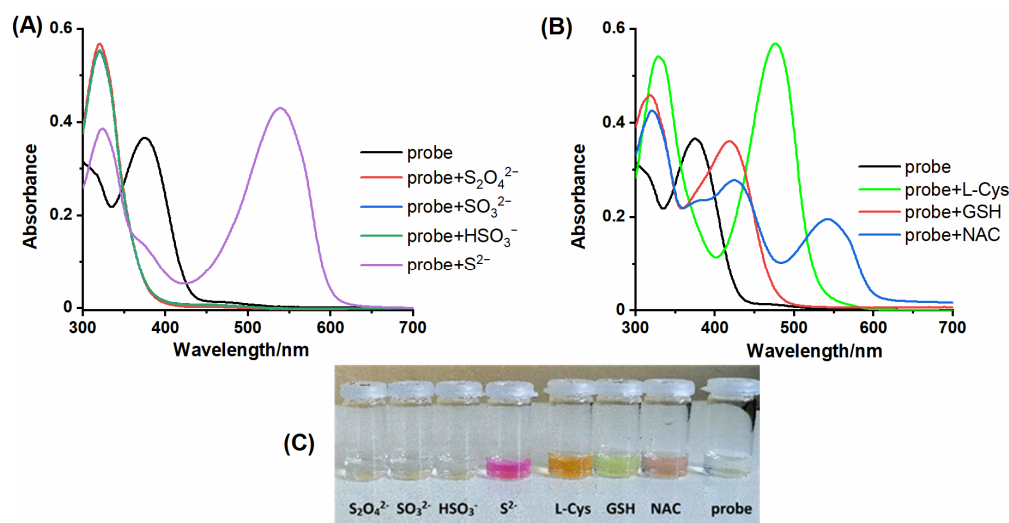


Figure 3. The UV-vis absorption spectra of probe NBD-O-CmCH₂OH (7.5 μM) upon the addition of 5 equivalents of various (A) sulfur species and (B) biothiols in MeCN-PB (1:9 *v/v*, pH 7.4). (C) Photograph of the probe in the presence of different analytes.

2.3. HPLC and Fluorescence Measurements

Over the last decade, it has been emphasized that fluorescent identification of analyte formed in cells is practically impossible without employing HPLC- or LC-MS-based methods to detect analyte-specific product(s) [39]. Therefore, we have developed HPLC-based methods to detect the specific reaction products of the NBD-O-CmCH₂OH probe with the tested thiols. Each of these reactions produces a fluorescent coumarin CmCH₂OH (retention time 1.95 min) and NBD-specific adducts: NBD-SH (2.99 min), NBD-GSH (2.50 min), NBD-NAC (3.25 min), and NBD-Cys (3.45 min) (Figure 4A). A comparison of the retention time of the authentic standards, which were obtained by reacting NBD-Cl with an appropriate biothiol, confirms that these NBD adducts are the only products found in the reaction mixture (Figure 4B). NBD-SH, NBD-GSH, and NBD-NAC are S-bound NBD adducts. The S-bound NBD product of L-Cys is unstable and, in the presence of an excess of L-Cys, can quickly change into the corresponding N-bound NBD product via a unique nucleophilic aromatic substitution-intramolecular Smiles rearrangement, which we show later in this work (Scheme 4). Using our probe in conjunction with the HPLC technique, we can detect the presence of specific biothiol in a mixture.

Next, we examined the stoichiometry of the probe reaction with the tested compounds. We used two methods to determine the reaction's stoichiometry between the probe and tested thiols. Initially, HPLC titration of NBD-O-CmCH₂OH with increasing concentration of Na₂S and studied biothiols were performed. Chromatograms (Figure 5A) show the slow disappearance of the probe (NBD-O-CmCH₂OH, *r*_t = 4.15 min) and the formation of a fluorescence product with a retention time of 1.95 min. A comparison of the retention time of the authentic standard of 7-hydroxy-4-(hydroxymethyl)-coumarin (CmCH₂OH) confirms that this coumarin is one of the products found in the reaction mixture. Our stoichiometric analysis (Figure 5B) showed that three equivalents of Na₂S completely consumed the NBD-O-CmCH₂OH probe.

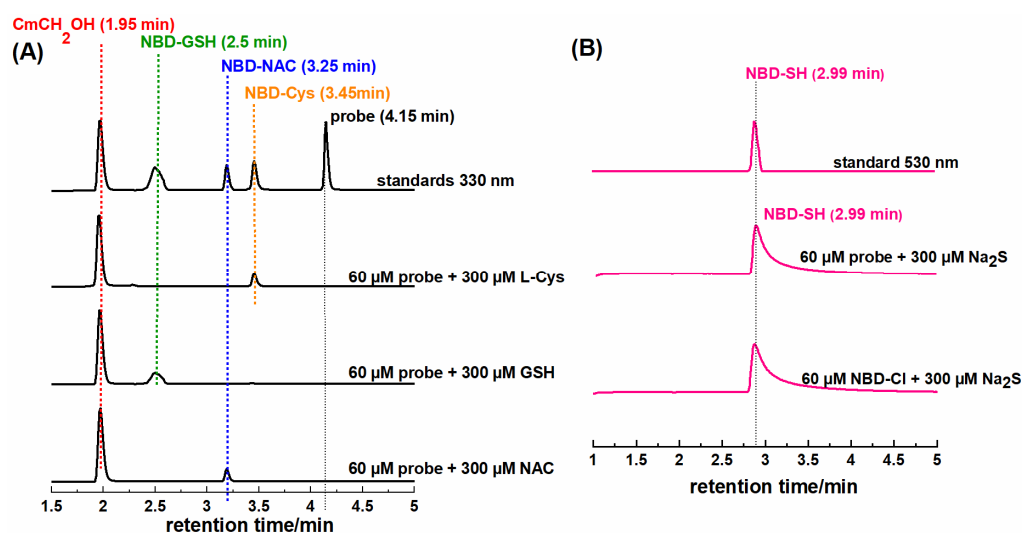
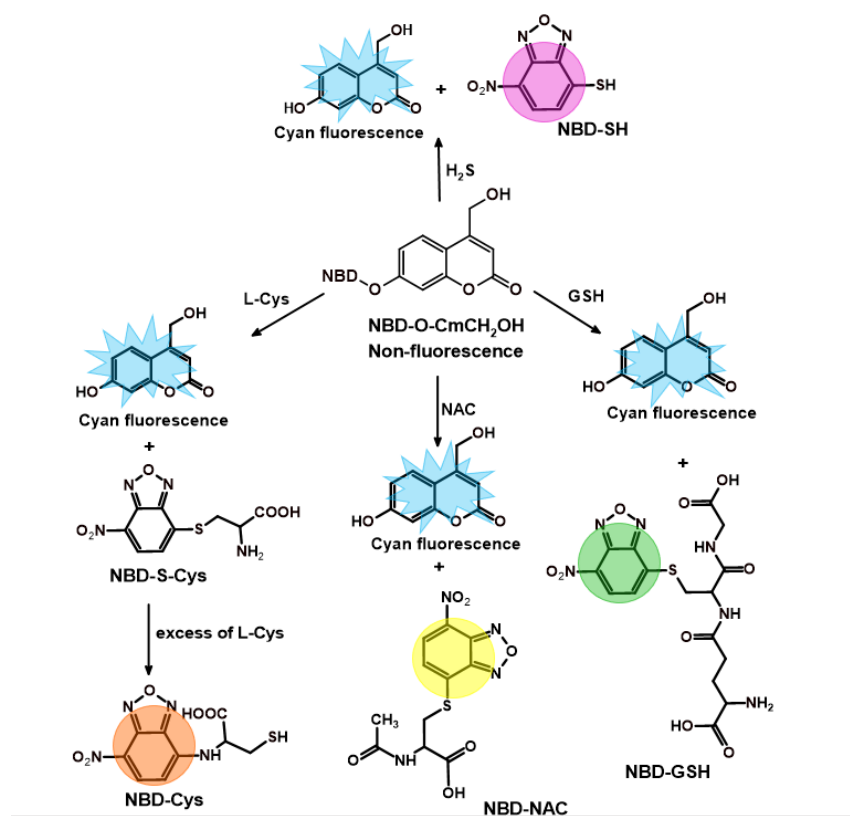


Figure 4. (A) HPLC chromatogram recorded at 330 nm of the standards and the reactions products of NBD-O-CmCH₂OH (60 μM) with various biothiols (each 300 μM). (B) HPLC chromatogram recorded at 530 nm of the NBD-SH standard and the reaction mixtures of probe and NBC-Cl (60 μM) with Na₂S (300 μM). The incubation time was 15 min.



Scheme 4. The proposed sensing mechanism of NBD-O-CmCH₂OH for H₂S, NAC, L-Cys, and GSH.

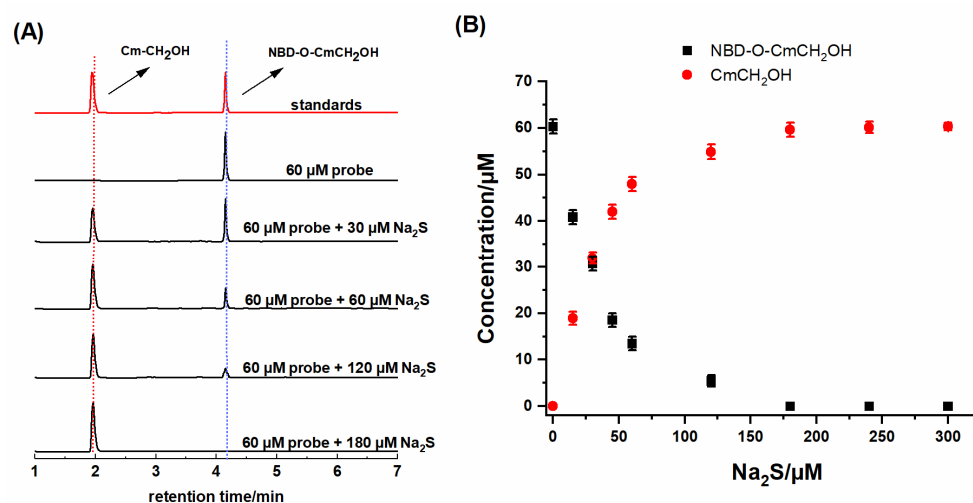


Figure 5. (A) HPLC chromatogram of the standards (60 μM) and reaction mixtures of NBD-O-CmCH₂OH (60 μM) with Na₂S (0–300 μM) after 15 min incubation. The traces were collected using an absorption detector set at 330 nm. (B) HPLC-based titration of NBD-O-CmCH₂OH (60 μM) with Na₂S after 15 min of incubation in solution. Data are means \pm standard deviation of three independent experiments.

In addition, the concentration-dependent fluorescence measurements of NBD-O-CmCH₂OH toward Na₂S, L-Cys, GSH, and NAC were performed. Recorded emission spectra showed gradual enhancement in fluorescence intensity at 473 nm with an increased concentration of biothiols (Figure 6). Using these fluorescence measurements, the detection limits (LOD = 3.3 σ /S) of NBD-O-CmCH₂OH for H₂S, L-Cys, GSH, and NAC were calculated on 140 nM, 26 nM, 60 nM, and 32 nM, respectively (Table 1). The dependence of the fluorescence intensity on the added thiol concentration shows that the emission of the probe reaches a maximum for various concentrations of Na₂S and biothiols. To get the emission plateau, four equivalents of Na₂S and one equivalent of biothiol are needed.

We also recorded HPLC chromatograms during the reaction of the NBD-O-CmCH₂OH probe with various biothiols (Figure 7). The stoichiometric analysis showed that all tested biothiols entirely consumed the NBD-derived probe. The maximum yield of CmCH₂OH was achieved when the probe was reacted with a slight excess of the biothiols consistent with the 1:1 or 1:2 stoichiometry. The probe reacting with 0.5 equivalent of L-Cys gives a fluorescent coumarin and a new product with a retention time of 4.5 min, which can be assigned to NBD-S-Cys. The stoichiometric amount of L-Cys caused a significant disappearance of this product and the formation of a proper NBD-Cys adduct with a retention time of 3.5 min. The addition of two equivalents of L-Cys caused the complete conversion of NBD-S-Cys to NBD-Cys (Figure 7A). These studies confirm that the S-bound NBD adduct of L-Cys can undergo intramolecular rearrangement under these conditions. Moreover, we do not observe any intermediate products during the probe's reaction with GSH or NAC (Figure 7B,C). These thiols could not induce this intramolecular rearrangement reaction due to the lack of a proximal NH₂ or blocked amino group. For better visualization of the formation of specific NBD adducts, we also recorded the HPLC chromatogram at 420 nm (Figure S5).

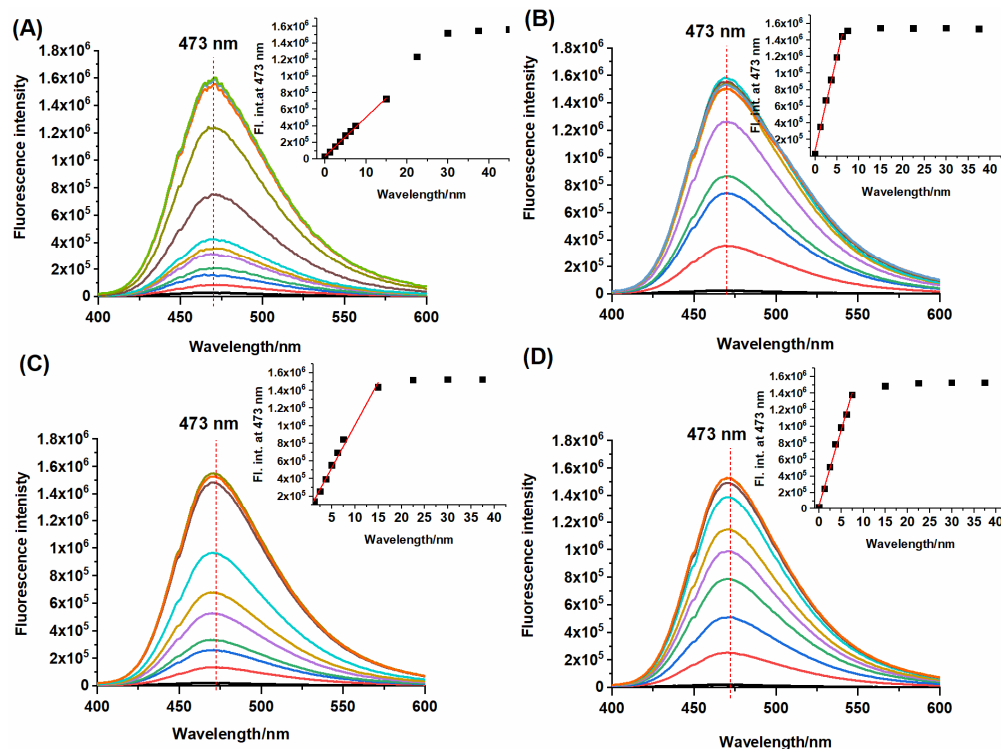


Figure 6. Emission spectra of probe NBD-O-CmCH₂OH (7.5 μM) in the presence of various concentrations of (A) Na₂S (0–45 μM), (B) L-Cys (0–37.5 μM), (C) GSH (0–37.5 μM), (D) NAC (0–37.5 μM) in phosphate buffer (0.1 M, pH 7.4, with 10% MeCN, *v/v*). Spectra were recorded after 10 min of incubation at room temperature.

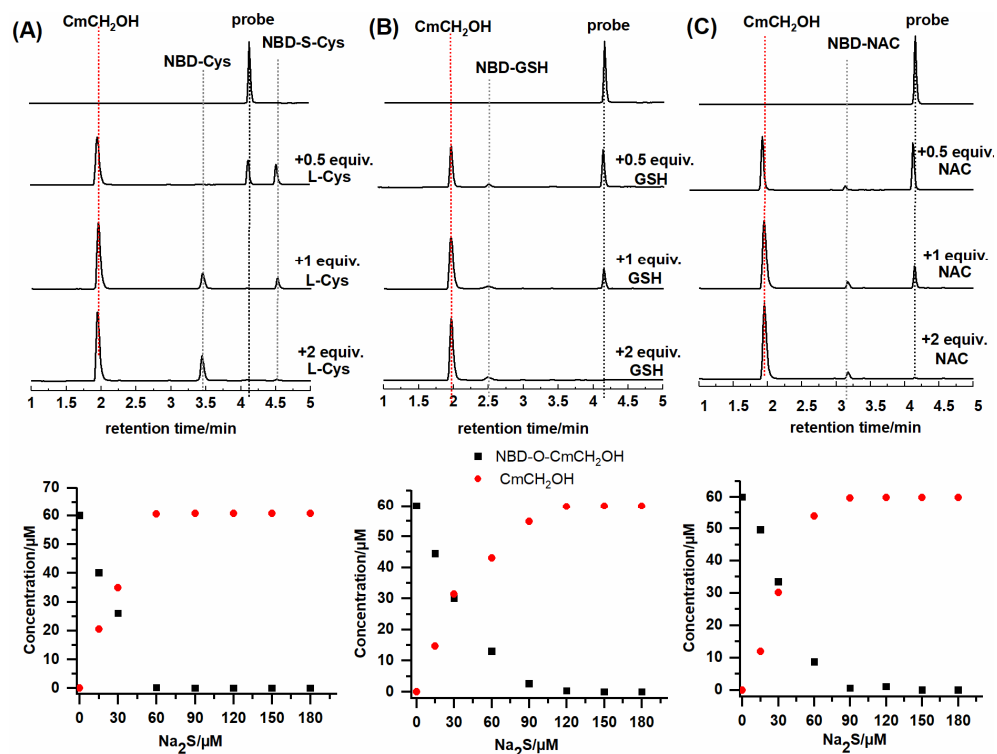


Figure 7. HPLC chromatogram and the HPLC based-titration of the reaction mixtures of NBD-O-CmCH₂OH (60 μM) with (A) L-Cys (0–180 μM), (B) GSH (0–180 μM), (C) NAC (0–180 μM) after 15 min incubation. The traces were collected using an absorption detector set at 330 nm.

3. Materials and Methods

3.1. Materials and Instruments

All reagents for synthesis were obtained from commercial suppliers and used without purification. Distilled water was used throughout all experiments. ^1H NMR and ^{13}C -NMR spectra were recorded with a Bruker Avance III 600 using as solvent DMSO- d_6 or CD_3OD . High-resolution mass spectra were taken on using Synapt G2-Si mass spectrometer equipped with an electrospray ionization (ESI) source and time of flight (TOF) analyzer. UV-vis absorption spectra were recorded on a Jasco V-670 spectrophotometer. Fluorescence spectra were recorded using FLS-920 (Edinburgh Instruments, UK) with excitation and emission slit widths of 1 nm. HPLC chromatograms were obtained using UFLC Shimadzu equipped with UV-Vis absorption and fluorescence detector. Analyses were done using a Kinetex C18 column (Phenomenex 100 mm \times 46 mm, 2.6 μm) equilibrated with 10% MeCN in water containing 0.1% trifluoroacetic acid (TFA).

3.2. Synthesis

The synthetic pathway starting from resorcinol toward NBD-O-CmCH₂OH is depicted in Scheme 2. The 4-chloromethyl-7-hydroxycoumarin (CmCH₂Cl) and 7-hydroxy-4-(hydroxymethyl)-2H-chromen-2-one (CmCH₂OH) were prepared according to a slightly modified procedure described elsewhere [48,49]. The following derivatives of NBD, such as NBD-SH, NBD-Cys, NBD-GSH, and NBD-NAC, were obtained by the straightforward synthesis depicted in Scheme 3.

3.2.1. Synthesis of 4-Chloromethyl-7-hydroxycoumarin (CmCH₂Cl)

A solution of resorcinol (3.30 g, 30 mmol) in ethyl 4-chloroacetoacetate (5.52 mL, 40 mmol) was added dropwise to cooled, concentrated sulfuric acid (20 mL) at 5 °C. Then the reaction mixture was stirred at room temperature for 2 h. The mixture was poured into ice water, and the precipitate was collected by suction filtration and washed with cold water, dried to afford pure CmCH₂Cl as a colorless solid (5.14 g, 82%), $R_f = 0.89$ (DCM:MeOH 17:3, *v/v*), m.p. 187–188 °C (186–188 °C [48]). ^1H NMR (DMSO- d_6 , 600 MHz) δ (ppm): 4.96 (2H, s); 6.42 (1H, s); 6.76 (1H, d, $J = 2.4$ Hz); 6.85 (1H, dd, $J_1 = 6.6$ Hz, $J_2 = 2.4$ Hz); 7.68 (1H, d, $J = 8.4$ Hz); 10.64 (1H, s); ^{13}C NMR (DMSO- d_6 , 151 MHz) δ (ppm): 41.8; 103.0; 109.8; 111.5; 113.6; 127.0; 151.4; 155.8; 160.6; 161.9; HRMS $[\text{M}-\text{H}]^-$ for $\text{C}_{10}\text{H}_6\text{ClO}_3$ 209.0005, found 209.0010.

3.2.2. Synthesis of 7-Hydroxy-4-(hydroxymethyl)-2H-chromen-2-one (CmCH₂OH)

CmCH₂Cl (1.5 g, 7 mmol) was added to water (100 mL). The reaction mixture was refluxed for 48 h, then filtered while hot and cooled to room temperature to yield a white precipitate. The product was filtered, washed with a large amount of cold water, and chromatographed on silica gel (DCM:MeOH 17:3, *v/v*) to give CmCH₂OH as a white solid ($R_f = 0.78$, 1.2 g, 89%), m.p. 213–217 °C (216–218 °C [49]). ^1H NMR (DMSO- d_6 , 600 MHz) δ (ppm): 4.71 (2H, s); 5.57 (1H, s); 6.25 (1H, s); 6.73 (1H, d, $J = 1.8$ Hz); 6.77 (1H, dd, $J_1 = 6.0$ Hz, $J_2 = 2.4$ Hz); 7.68 (1H, d, $J = 8.4$ Hz); ^{13}C NMR (DMSO- d_6 , 151 MHz) δ (ppm): 59.5; 102.8; 107.1; 110.1; 113.3; 125.9; 155.4; 157.2; 161.1; 161.5; HRMS $[\text{M}-\text{H}]^-$ for $\text{C}_{10}\text{H}_7\text{O}_4$ 191.0344, found 191.0343.

3.2.3. Synthesis of 7-Nitrobenzofurazan Ether-4-Hydroxymethylcoumarin (NBD-O-CmCH₂OH)

CmCH₂OH (0.15g, 0.78 mmol) and triethylamine (0.22 mL, 1.6 mmol) were dissolved in anhydrous ethanol (30 mL), and next, NBD-Cl (0.16 g, 0.8 mmol) was added in one portion to the flask, and the resulting mixture was stirred at room temperature for 8 h. After removal of the solvent, the residue was chromatographed on silica gel using DCM:MeOH (17:3, *v/v*) to afford pure NBD-O-CmCH₂OH as a yellow solid ($R_f = 0.85$ (DCM:MeOH 17:3, *v/v*), 0.19 g, 69%), m.p. 215–217 °C. ^1H NMR (DMSO- d_6 , 600 MHz) δ (ppm): 4.81 (2H, s); 5.73 (1H, s); 6.51 (1H, s); 7.02 (1H, d, $J = 8.4$ Hz); 7.42 (1H, dd, $J_1 = 6.6$ Hz, $J_2 = 2.4$ Hz); 7.91

(1H, d, J = 9.0 Hz); 8.68 (1H, d, J = 8.4 Hz); ¹³C NMR (DMSO-*d*₆, 151 MHz) δ (ppm): 59.6; 109.3; 110.9; 112.3; 116.2; 117.1; 127.2; 131.7; 135.6; 144.9; 145.9; 152.2; 154.8; 156.0; 156.5; 160.2; HRMS [M + H]⁺ for C₁₆H₁₀N₃O₇ = 356.0519, found 356.0528.

3.2.4. Synthesis of 7-Nitrobenzo[c][1,2,5]oxadiazole-4-thiol (NBD-SH)

4-Chloro-7-nitrobenzo[c][1,2,5]oxadiazole (NBD-Cl, 0.1 g, 0.5 mmol) was dissolved in 5 mL of MeOH. Next, anhydrous Na₂S (0.078 g, 1 mmol) was dissolved in 5 mL of MeOH and slowly added to the solution of NBD-Cl. The reaction mixture changed from yellow to deep purple and was stirred at room temperature for 30 min. Next, the MeOH was removed under a vacuum to afford the desired product as dark purple powder. The final product was purified by chromatography on SiO₂ using DCM:MeOH (17:3, *v/v*) (0.079 g, 82%). ¹H NMR (DMSO-*d*₆, 600 MHz) δ (ppm): 5.75 (1H, d, J = 9.6 Hz); 8.25 (1H, d, J = 10.2 Hz); ¹³C NMR (DMSO-*d*₆, 151 MHz) δ (ppm): 111.5; 115.6; 123.1; 138.3; 147.2; 148.6; HRMS [M-H]⁻ for C₆H₂N₃O₃S: 195.9817, found 195.9820.

3.2.5. Synthesis of 4-Nitrobenz-2-oxa-1,3-diazole (NBD) Derived Compounds: NBD-Cys, NBD-GSH, NBD-NAC

NBD-Cl (0.15 g, 0.7 mmol) and triethylamine (0.146 mL, 1.05 mmol) were added to EtOH (20 mL), and then a solution of proper biothiol (1.4 mmol) in 5 mL of water was added to the flask. The resulting mixture was stirred for 3h at room temperature. The resulting precipitate was filtered and washed with cold ethanol to give a crude product which was then purified by chromatography on SiO₂ using DCM:MeOH (17:3, *v/v*).

NBD-Cys (cysteine derivative): orange solid, yield 85%; ¹H NMR (CD₃OD, 600 MHz) δ (ppm): 3.66 (1H, br. s); 4.55 (2H, br. s); 6.42 (1H, d, J = 9.0 Hz); 8.52 (1H, d, J = 8.4 Hz); HRMS [M-H]⁻ for C₉H₇N₄O₅S: 283.0137 found 283.0141.

NBD-GSH (glutathione derivative): yellow solid, yield 68%; ¹H NMR (DMSO-*d*₆, 600 MHz) δ (ppm): 1.90–1.98 (2H, m); 2.36 (2H, t, J = 7.2 Hz); 3.38 (2H, t, J = 6.0 Hz); 3.53–3.57 (2H, m); 3.76–3.80 (2H, m); 4.72–4.75 (2H, m); 7.64 (1H, d, J = 8.4 Hz); 8.59 (1H, d, J = 7.8 Hz); 8.75; 8.81 (2H, d-like); ¹³C NMR (DMSO-*d*₆, 151 MHz) δ (ppm): 27.1; 31.8; 33.5; 41.8; 51.6; 53.5; 123.1; 132.8; 132.9; 139.6; 143.1; 149.6; 170.2; 171.1; 171.3; 173.8; HRMS [M-H]⁻ for C₁₆H₁₇N₆O₉S: 469.0778, found 469.0785.

NBD-NAC (*N*-acetylcysteine derivative): brown solid, yield 73%; ¹H NMR (DMSO-*d*₆, 600 MHz) δ (ppm): 1.87 (3H, s); 2.53 (2H, d-like); 4.66 (1H, d-like); 7.60 (1H, d, J = 6.6 Hz); 8.53 (1H, d, J = 6.6 Hz); 8.60 (1H, d, J = 6.6 Hz); ¹³C NMR (DMSO-*d*₆, 151 MHz) δ (ppm): 22.8; 33.0; 52.1; 123.3; 132.8; 133.0; 139.3; 143.1; 149.7; 170.1; 171.7; HRMS [M-H]⁻ for C₁₁H₉N₄O₆S: 325.0243, found 325.0244.

3.3. UV-Vis, Fluorescent, and HPLC Analysis

All spectroscopic measurements were performed in phosphate buffer (0.1 M, pH 7.4) containing 10% MeCN at room temperature. Probe NBD-O-CmCH₂OH and fluorescent standard CmCH₂OH were dissolved in MeCN to prepare 1 mM solutions. Before each experiment probe was diluted with phosphate buffer (0.1 M, pH 7.4 with 10% MeCN) to afford the final concentration. Sodium sulfide (Na₂S) was selected as a H₂S donor. The stock solution of Na₂S (1 mM) in PB buffer (0.1 M, pH 7.4) was always prepared before experiments. To evaluate hydrogen sulfide concentration in phosphate buffer, we used Ellman's reagent, i.e., 5,5'-dithiobis(2-nitrobenzoic acid (DTNB), and a detailed procedure is described in our previous paper [39]. Aqueous stock solutions (1 mM) of an amino acid (Cys, GSH, NAC) and sodium salts (SO₄²⁻, S₂O₄²⁻, SO₃²⁻, HSO₃⁻) were prepared using deionized water. All measurements were performed in a 3.5 mL quartz cuvette with a 2 mL solution. The reaction mixture was shaken uniformly at room temperature before recording spectra. For fluorescence measurement, the excitation wavelength was set at 320 nm. The adjustment slit was 1 nm/1 nm for each fluorescence measurement. The standards and products formed in the reaction of NBD-O-CmCH₂OH with H₂S and tested biothiols were eluted by an increase of MeCN concentration from 10 to 100% over 12 min

at the flow rate of 1.5 mL/min. The HPLC trace of NBD-O-CmCH₂OH and CmCH₂OH formed in reaction with H₂S was detected by monitoring the absorption at 330 nm. HPLC traces of NBD-SH and NBD-Cys, NBD-GSH, and NBD-NAC were detected by monitoring absorption at 530 nm and 420 nm, respectively.

4. Conclusions

In the current investigations, a coumarin analog fluorescent probe has been applied to indicate the hydrogen sulfide and the naturally occurring biothiols (cysteine, *N*-acetylcysteine, and glutathione). The design and synthesis were described, and the NBD-derived probe was reacted with H₂S, L-Cys, NAC, and GSH to show similar rate constants. The differences in the stoichiometry of the probe response to H₂S, GSH, L-Cys, and NAC are reflected in the detection limits. The probe's ether bond cleavage by the corresponding biothiol releases the coumarin fluorophore and produces thiol-NBD adducts. The appropriate NBD-derived products with H₂S, Cys, NAC, and GSH possess various colors and retention times that distinguish those biological thiols. We also confirmed that intramolecular rearrangement is only possible for the adduct formed during the reaction of the probe NBD-O-CmCH₂OH with L-Cys. The resulting NBD-S-Cys cleavage product can rapidly transform to create a new NBD-Cys adduct only when excess L-Cysteine is used.

Supplementary Materials: The following are available online at <https://www.mdpi.com/article/10.3390/molecules27238305/s1>, The document provides additional data, including ¹H, ¹³C NMR, HRMS spectra, spectrophotometric, and HPLC study [45,53–59].

Author Contributions: Conceptualization, D.S.; methodology, D.S. and R.P.; formal analysis, D.S.; investigation, D.S. and M.Ś.; resources, D.S. and R.P.; writing—original draft preparation, D.S.; writing—review and editing, R.P. and J.R.; supervision, R.P. All authors have read and agreed to the published version of the manuscript.

Funding: This work was supported by the National Center for Research and Development (Warsaw, Poland) within the grant InterChemMed (POWR.03.02.00–00-I029/16).

Institutional Review Board Statement: Not applicable.

Informed Consent Statement: Not applicable.

Data Availability Statement: Not applicable.

Conflicts of Interest: The authors declare no conflict of interest.

Sample Availability: Samples of the all synthesized compounds are available from the authors.

Abbreviations

H ₂ S	hydrogen sulfide
NAC	<i>N</i> -acetylcysteine
GSH	glutathione
Cys	L-Cysteine
NBD-Cl	4-Chloro-7-nitrobenzo[c][1,2,5]oxadiazole
NBD-GSH	7-nitrobenzo[c][1,2,5]oxadiazole-4-glutathione
NBD-NAC	<i>N</i> -acetyl-S-(7-nitrobenzo[c][1,2,5]oxadiazol-4-yl)cysteine
NBD-Cys	7-nitrobenzo[c][1,2,5]oxadiazole-4-cysteine
CmCH ₂ Cl	4-chloromethyl-7-hydroxycoumarin
CmCH ₂ OH	7-hydroxy-4-(hydroxymethyl)-2H-chromen-2-one
NBD-O-CmCH ₂ OH	7-nitrobenzofurazan ether-4-hydroxymethylcoumarin
MeCN	acetonitrile
PB buffer	phosphate buffer
Na ₂ S	sodium sulfide

References

1. Zhu, H.; Liu, C.; Zhang, H.; Jia, P.; Li, Z.; Zhang, X.; Yu, Y.; Sheng, W.; Zhu, B. A Simple Long-wavelength Fluorescent Probe for Simultaneous Discrimination of Cysteine/Homocysteine and Glutathione/Hydrogen Sulfide with Two Separated Fluorescence Emission Channels by Single Wavelength Excitation. *Anal. Sci.* **2020**, *36*, 255–262. [[CrossRef](#)] [[PubMed](#)]
2. Qi, X.; Shang, L.; Liang, S.; Li, H.; Chen, J.; Xin, C.; Zhao, J.; Deng, M.; Wang, Q.; He, Q.; et al. Development and applications of a coumarin-based “turn-on” fluorescent probe for effectively discriminating reduced glutathione from homocysteine and cysteine in living cells and organisms. *Dyes Pigments* **2021**, *194*, 109625. [[CrossRef](#)]
3. Zhang, X.; Jin, X.; Zhang, C.; Zhong, H.; Zhu, H. A fluorescence turn-on probe for hydrogen sulfide and biothiols based on PET & TICT and its imaging in HeLa cells. *Spectrochim. Acta Part A Mol. Biomol. Spectrosc.* **2021**, *244*, 118839. [[CrossRef](#)]
4. Lv, L.; Luo, W.; Diao, Q. A novel ratiometric fluorescent probe for selective detection and imaging of H₂S. *Spectrochim. Acta Part A Mol. Biomol. Spectrosc.* **2021**, *246*, 118959. [[CrossRef](#)] [[PubMed](#)]
5. Zhang, J.; Wen, G.; Wang, W.; Cheng, K.; Guo, Q.; Tian, S.; Liu, C.; Hu, H.; Zhang, Y.; Zhang, H.; et al. Controllable Cleavage of C–N Bond-Based Fluorescent and Photoacoustic Dual-Modal Probes for the Detection of H₂S in Living Mice. *ACS Appl. Bio Mater.* **2021**, *4*, 2020–2025. [[CrossRef](#)] [[PubMed](#)]
6. Szabo, C.; Papapetropoulos, A. International Union of Basic and Clinical Pharmacology. CII: Pharmacological Modulation of H₂S Levels: H₂S Donors and H₂S Biosynthesis Inhibitors. *Pharmacol. Rev.* **2017**, *69*, 497–564. [[CrossRef](#)] [[PubMed](#)]
7. Han, Y.; Shang, Q.; Yao, J.; Ji, Y. Hydrogen sulfide: A gaseous signaling molecule modulates tissue homeostasis: Implications in ophthalmic diseases. *Cell Death Dis.* **2019**, *10*, 293. [[CrossRef](#)] [[PubMed](#)]
8. Hao, Y.; Wang, H.; Fang, L.; Bian, J.; Gao, Y.; Li, C. H₂S Donor and Bone Metabolism. *Front. Pharmacol.* **2021**, *12*, 661601. [[CrossRef](#)] [[PubMed](#)]
9. Sun, Q.; Liu, H.; Qiu, Y.; Chen, J.; Wu, F.; Luo, X.; Wang, D. A highly sensitive and selective fluorescence turn-on probe for the sensing of H₂S in vitro and in vivo. *Spectrochim. Acta Part A Mol. Biomol. Spectrosc.* **2021**, *254*, 119620. [[CrossRef](#)]
10. Zivanovic, J.; Filipovic, M. Hydrogen sulfide: Stench from the past as a mediator of the future. *Biochemist* **2016**, *38*, 12–17. [[CrossRef](#)]
11. Wang, R. Physiological Implications of Hydrogen Sulfide: A Whiff Exploration That Blossomed. *Physiol. Rev.* **2012**, *92*, 791–896. [[CrossRef](#)] [[PubMed](#)]
12. Coletta, C.; Papapetropoulos, A.; Erdelyi, K.; Olah, G.; Módis, K.; Panopoulos, P.; Asimakopoulou, A.; Gerö, D.; Sharina, I.; Martin, E. Hydrogen sulfide and nitric oxide are mutually dependent in the regulation of angiogenesis and endothelium-dependent vasorelaxation. *Proc. Natl. Acad. Sci. USA* **2012**, *109*, 9161–9166. [[CrossRef](#)] [[PubMed](#)]
13. Yang, Q.; Zhou, L.; Peng, L.; Yuan, G.; Ding, H.; Tan, L.; Zhou, Y. A smart mitochondria-targeting TP-NIR fluorescent probe for the selective and sensitive sensing of H₂S in living cells and mice. *New J. Chem.* **2021**, *45*, 7315–7320. [[CrossRef](#)]
14. Li, H.; Yao, Q.; Fan, J.; Jiang, N.; Wang, J.; Xia, J.; Peng, X. A fluorescent probe for H₂S in vivo with fast response and high sensitivity. *Chem. Commun.* **2015**, *51*, 16225–16228. [[CrossRef](#)]
15. Ma, Y.; Xu, Z.; Sun, Q.; Wang, L.; Liu, H.; Yu, F. A semi-naphthorhodafluor-based red-emitting fluorescent probe for tracking of hydrogen polysulfide in living cells and zebrafish. *Spectrochim. Acta Part A Mol. Biomol. Spectrosc.* **2021**, *247*, 119105. [[CrossRef](#)] [[PubMed](#)]
16. Calvert, J.; Jha, S.; Gundewar, S.; Elrod, J.; Ramachandran, A.; Pattillo, C.; Kevil, C.; Lefer, D. Hydrogen Sulfide Mediates Cardioprotection Through Nrf₂ Signaling. *Circ. Res.* **2009**, *105*, 365–374. [[CrossRef](#)] [[PubMed](#)]
17. Takano, Y.; Shimamoto, K.; Hanaoka, K. Chemical tools for the study of hydrogen sulfide (H₂S) and sulfane sulfur and their applications to biological studies. *J. Clin. Biochem. Nutr.* **2016**, *58*, 7–15. [[CrossRef](#)] [[PubMed](#)]
18. Kimura, H. Hydrogen sulfide as a neuromodulator. *Mol. Neurobiol.* **2002**, *26*, 13–19. [[CrossRef](#)]
19. Xiao, Q.; Ying, J.; Xiang, L.; Zhang, C. The biologic effect of hydrogen sulfide and its function in various diseases. *Medicine* **2018**, *97*, e13065. [[CrossRef](#)]
20. Wang, H.; Wu, X.; Yang, S.; Tian, H.; Liu, Y.; Sun, B. A dual-site fluorescent probe for separate detection of hydrogen sulfide and bisulfite. *Dyes Pigments* **2019**, *160*, 757–764. [[CrossRef](#)]
21. Feng, S.; Xia, Q.; Feng, G. Iminocoumarin-based red to near-infrared fluorescent turn-on probe with a large Stokes shift for imaging H₂S in living cells and animals. *Dyes Pigments* **2019**, *163*, 447–453. [[CrossRef](#)]
22. Hong, J.; Zhou, E.; Gong, S.; Feng, G. A red to near-infrared fluorescent probe featuring a super large Stokes shift for light-up detection of endogenous H₂S. *Dyes Pigments* **2019**, *160*, 787–793. [[CrossRef](#)]
23. Zhang, H.; Lin, Y.; Ma, Y.; Zhang, J.; Wang, C.; Zhang, H. Protective effect of hydrogen sulfide on monocrotaline induced pulmonary arterial hypertension via inhibition of the endothelial mesenchymal transition. *Int. J. Mol. Med.* **2019**, *44*, 2091–2102. [[CrossRef](#)]
24. Shen, F.; Zhao, C.; Shen, M.; Wang, Z.; Chen, G. The role of hydrogen sulfide in gastric mucosal damage. *Med. Gas. Res.* **2019**, *9*, 88–92. [[CrossRef](#)] [[PubMed](#)]
25. Ma, T.; Huo, F.; Yin, C. A ‘naked-eye’ ratiometric and NIR fluorescent detection for hydrogen sulphide with quick response and high selectivity for and its bioimaging. *Dyes Pigments* **2019**, *165*, 31–37. [[CrossRef](#)]
26. Zhang, H.; Zhu, M.; Jiang, D.; Xue, X.; Zhang, J.; Zhang, G.; Wang, Y.; Zhao, H. Ultrafast response fluorescent probe with red-emission for monitoring hydrogen sulfide in vivo and in vitro. *J. Photochem. Photobiol. A* **2019**, *382*, 111974. [[CrossRef](#)]

27. Guo, F.; Han, X.; Zhao, X.; Wang, Y.; Fan, Y.; Wu, W.; Xu, Z. A ratiometric fluorescent probe for hydrogen sulfide in neat aqueous solution and its application in lysosome-targetable cell imaging. *Spectrochim. Acta Part A Mol. Biomol. Spectrosc.* **2022**, *270*, 120835. [[CrossRef](#)]
28. Chen, X.; Mei, Y.; Li, H.; Song, Q. Rapid and sensitive detection of H₂S by a 4-phenylselenium coumarin as a dual-active-site fluorescent probe. *Sens. Actuators B Chem.* **2022**, *354*, 131202. [[CrossRef](#)]
29. Cuiling, S.; Huayu, W.; Tianjun, N.; Kaiwen, C.; Chunpo, G. A dicyanoisophorone-based near-infrared fluorescent probe with fast detection for H₂S in living cells and zebrafish. *J. Lumin.* **2022**, *243*, 118669. [[CrossRef](#)]
30. Jothi, D.; Iyer, S. A highly sensitive naphthalimide based fluorescent “turn-on” sensor for H₂S and its bio-imaging applications. *J. Photochem. Photobiol. A* **2022**, *427*, 113802. [[CrossRef](#)]
31. Ubuka, T.; Abe, T.; Kajikawa, R.; Morino, K. Determination of hydrogen sulfide and acid-labile sulfur in animal tissues by gas chromatography and ion chromatography. *J. Chromatogr. B* **2001**, *757*, 31–37. [[CrossRef](#)] [[PubMed](#)]
32. Ibrahim, H.; Serag, A.; Farag, M. Emerging analytical tools for the detection of the third gasotransmitter H₂S, a comprehensive review. *J. Adv. Res.* **2021**, *27*, 137–153. [[CrossRef](#)] [[PubMed](#)]
33. Liu, J.; Sun, Y.; Zhang, J.; Yang, T.; Cao, J.; Zhang, L.; Guo, W. A Ratiometric Fluorescent Probe for Biological Signaling Molecule H₂S: Fast Response and High Selectivity. *Chem. Eur. J.* **2013**, *19*, 4717–4722. [[CrossRef](#)]
34. Xiang, K.; Liu, Y.; Li, C.; Tian, B.; Tong, T.; Zhang, J. A colorimetric and ratiometric fluorescent probe with a large stokes shift for detection of hydrogen sulfide. *Dyes Pigments* **2015**, *123*, 78–84. [[CrossRef](#)]
35. Wang, M.; Li, K.; Hou, J.; Wu, M.; Huang, Z.; Yu, X. BINOL-Based Fluorescent Sensor for Recognition of Cu(II) and Sulfide Anion in Water. *J. Org. Chem.* **2012**, *77*, 8350–8354. [[CrossRef](#)] [[PubMed](#)]
36. Lu, X.; Wu, M.; Wang, S.; Qin, J.; Li, P. Synthesis and preliminary exploration of a NIR fluorescent probe for the evaluation of androgen dependence of prostate cancer. *Talanta* **2022**, *239*, 123058. [[CrossRef](#)] [[PubMed](#)]
37. Zhang, K.; Meng, J.; Bao, W.; Liu, M.; Wang, X.; Tian, Z. Mitochondrion-targeting near-infrared fluorescent probe for detecting intracellular nanomolar level hydrogen sulfide with high recognition rate. *Anal. Bioanal. Chem.* **2021**, *413*, 1215–1224. [[CrossRef](#)]
38. Chao, W.; Qing, Z.; Weiwei, L.; Wenbin, C.; Zhen, X.; Long, Y. NBD-based colorimetric and fluorescent turn-on probes for hydrogen sulfide. *Org. Biomol. Chem.* **2014**, *12*, 479–485. [[CrossRef](#)]
39. Słowiński, D.; Świerczyńska, M.; Grzelakowska, A.; Szala, M.; Kolińska, J.; Romański, J.; Podsiadły, R. Hymecromone naphthoquinone ethers as probes for hydrogen sulfide detection. *Dyes Pigments* **2021**, *196*, 109765. [[CrossRef](#)]
40. Lin, V.; Chen, W.; Xian, M.; Chang, C. Chemical Probes for Molecular Imaging and Detection of Hydrogen Sulfide and Reactive Sulfur Species in Biological Systems. *Chem. Soc. Rev.* **2015**, *44*, 4596–4618. [[CrossRef](#)]
41. Świerczyńska, M.; Słowiński, D.; Grzelakowska, A.; Szala, M.; Romański, J.; Pierzchała, K.; Siarkiewicz, P.; Michalski, R.; Podsiadły, R. Selective, stoichiometric and fast-response fluorescent probe based on 7-nitrobenz-2-oxa-1,3-diazole fluorophore for hypochlorous acid detection. *Dyes Pigments* **2021**, *193*, 109563. [[CrossRef](#)]
42. Ding, S.; Feng, G. Smart probe for rapid and simultaneous detection and discrimination of hydrogen sulfide, cysteine/homocysteine, and glutathione. *Sens. Actuators B Chem.* **2016**, *235*, 691–697. [[CrossRef](#)]
43. Bae, J.; Choi, J.; Park, T.; Chang, S. Reaction-based colorimetric and fluorogenic signaling of hydrogen sulfide using a 7-nitro-2,1,3-benzoxadiazole–coumarin conjugate. *Tetrahedron Lett.* **2014**, *55*, 1171–1174. [[CrossRef](#)]
44. Zhai, L.; Shi, Z.; Tu, Y.; Pu, S. A dual emission fluorescent probe enables simultaneous detection and discrimination of Cys/Hcy and GSH and its application in cell imaging. *Dyes Pigments* **2019**, *165*, 164–171. [[CrossRef](#)]
45. Chen, W.; Luo, H.; Liu, X.; Foley, J.W.; Song, X. Broadly applicable Strategy for the fluorescence based detection and differentiation of glutathione and cysteine/homocysteine: Demonstration in vitro and in vivo. *Anal. Chem.* **2016**, *88*, 3638–3646. [[CrossRef](#)] [[PubMed](#)]
46. Men, Y.; Li, Z.; Zhang, J.; Tong, Z.; Xi, Z.; Qiu, X.; Yi, L. Rational design and synthesis of fast-response NBD-based fluorescent probes for biothiols. *Tetrahedron Lett.* **2015**, *56*, 5781–5786. [[CrossRef](#)]
47. Hammers, M.; Pluth, M. Ratiometric Measurement of Hydrogen Sulfide and Cysteine/Homocysteine Ratios Using a Dual-Fluorophore Fragmentation Strategy. *Anal. Chem.* **2014**, *86*, 7135–7140. [[CrossRef](#)]
48. Goud, N.; Makani, V.; Pranay, J.; Alvala, R.; Qureshi, I.; Kumar, P.; Bharath, R.; Nagaraj, C.; Yerramsetty, S.; Pal-Bhadra, M.; et al. Synthesis, 18F-radiolabeling and apoptosis inducing studies of novel 4, 7-disubstituted coumarins. *Bioorg. Chem.* **2020**, *97*, 103663. [[CrossRef](#)] [[PubMed](#)]
49. Ji, W.; Liu, G.; Wang, F.; Zhub, Z.; Feng, C. Galactose-decorated light-responsive hydrogelator precursors for selectively killing cancer cells. *Chem. Commun.* **2016**, *52*, 12574. [[CrossRef](#)]
50. Carballal, S.; Trujillo, M.; Cuevasanta, E.; Bartesaghi, S.; Möller, M.; Folkes, L.; García-Bereguiaín, M.; Gutiérrez-Merino, C.; Wardman, P.; Denicola, A.; et al. Reactivity of hydrogen sulfide with peroxynitrite and other oxidants of biological interest. *Free Radic. Biol. Med.* **2011**, *50*, 196–205. [[CrossRef](#)]
51. Tummanapelli, A.; Vasudevan, S. Initio MD Simulations of the Brønsted Acidity of Glutathione in Aqueous Solutions: Predicting pKa Shifts of the Cysteine Residue. *J. Phys. Chem. B* **2015**, *119*, 15353–15358. [[CrossRef](#)] [[PubMed](#)]
52. Fazary, A.; Awwad, N.; Ibrahim, H.; Shati, A.; Alfaifi, M.; Ju, Y. Protonation Equilibria of N-Acetylcysteine. *ACS Omega* **2020**, *5*, 19598–19605. [[CrossRef](#)]
53. Zhang, Y.; Wang, J.; Yue, J.; Chao, J.; Huo, F.; Yin, C. A new strategy for the fluorescence discrimination of Cys/Hcy and GSH/H₂S simultaneously colorimetric detection for H₂S. *Spectrochim. Acta A Mol. Biomol.* **2020**, *227*, 117537. [[CrossRef](#)] [[PubMed](#)]

54. Zhu, H.; Liu, C.; Yuan, R.; Wang, R.; Zhang, H.; Li, Z.; Jia, P.; Zhu, B.; Sheng, W. A simple highly specific fluorescent probe for simultaneous discrimination of cysteine/ homocysteine and glutathione/hydrogen sulfide in living cells and zebrafish using two separated fluorescence channels under single wavelength excitation. *Analyst* **2019**, *144*, 4258. [[CrossRef](#)] [[PubMed](#)]
55. Liu, T.; Li, S.; Zhang, X.; Wang, J.; Deng, Y.; Sun, X.; Xing, Z.; Wu, R. A facile probe for fluorescence turn-on and simultaneous naked-eyes discrimination of H₂S and biothiols (Cys and GSH) and its application. *J. Fluoresc.* **2022**, *32*, 175–188. [[CrossRef](#)]
56. Hao, Y.; Zhang, Y.; Zhu, D.; Luo, L.; Chen, L.; Tang, Z.; Zeng, R.; Xu, M.; Chen, S. Dual-emission fluorescent probe for discriminative sensing of biothiols. *Chinese J. Anal. Chem.* **2022**, *50*, 100153. [[CrossRef](#)]
57. Yang, Y.; Xu, Z.; Han, L.; Fan, Y.; Qing, M.; Li, N.; Luo, H. A simple fluorescent probe with two different fluorescence signals for rapid sequence distinguishing of Cys/Hcy/GSH and intracellular imaging. *Dye. Pigment.* **2021**, *184*, 108722. [[CrossRef](#)]
58. Xu, S.; Zhou, J.; Dong, X.; Zhao, W.; Zhu, Q. Fluorescent probe for sensitive discrimination of Hcy and Cys/GSH in living cells via dual-emission. *Anal. Chim. Acta* **2019**, *1074*, 123–130. [[CrossRef](#)] [[PubMed](#)]
59. Niu, H.; Duan, Y.; Zhang, Y.; Hua, X.; Xu, C.; Li, Z.; Ma, J.; Qin, F.; Zhai, Y.; Ye, Y.; et al. A bifunctional fluorescent probe based on PET & ICT for simultaneously recognizing Cys and H₂S in living cells. *J. Photochem. Photobiol. B Biol.* **2022**, *230*, 112441.